Computers and Electronics in Agriculture 166 (2019) 104975

Contents lists available at ScienceDirect

Computers and Electronics in Agriculture

journal homepage: www.elsevier.com/locate/compag

Apple tree canopy leaf spatial location automated extraction based on point cloud data

Cailing Guo[a,b,c], Gang Liu[a,b,*], Weijie Zhang[a,b], Juan Feng[d]

[a] Key Laboratory of Modern Precision Agriculture System Integration Research, Ministry of Education, China Agricultural University, Beijing 100083, China
[b] Key Lab of Agricultural Information Acquisition Technology, Ministry of Agricultural and Rural Affairs, China Agricultural University, Beijing 100083, China
[c] Department of Electromechanical Engineering, Tangshan University, Tangshan 063000, China
[d] College of Information Science & Technology, He Bei Agricultural University, Baoding 071001, China

ARTICLE INFO

Keywords:
Terrestrial laser scanning
Apple tree canopy
Leaf spatial location
Automated extraction
Point cloud

ABSTRACT

A fine structure inside the canopy of the apple tree determines the light distribution and is one of the important factors affecting the quality and yield of apples. Leaf spatial location (LSL) is the spatial co-ordinates of the petiole–midrib junction point. In this paper, a Trimble TX8 was used to obtain 3D point clouds of the canopy in the flowering, leaf growth stage and stable growth stages of apple tree as the research object. An LSL extraction approach using density-based spatial clustering of applications with noise (DBSCAN) and layers K-mean and median (L-KaM) methods was proposed. Firstly, the DBSCAN clustering method based on adaptive parameters is used to separate single leaves from branches. Secondly, the same point cloud is sliced into layers, and the L-KaM method is used to fit the branch center line. Finally, the Euclidean distance of each point between the single leaf and the center line is determined, and the point with the smallest Euclidean distance is the LSL point. Field experiments show that the DBSCAN-L-KaM method proposed in this study is suitable for LSL extraction during the leaf growth and stable growth stages. The maximum Euclidean distance between the manual measurements' actual LSL value and the values automatically extracted (ELD_MaA) was less than 9 mm, and the average ELD_MaA was 1.41 mm. The average extraction rate of tall spindle training system apple trees and free spindle training system apple trees were 89.90% and 51.75%, respectively. Using the method in this paper, we obtain the whole apple tree (3-year-old) LSL value in about 2.5–3 h. The method provides theoretical basis and systemic support for the analysis of the light-intensity distribution of apple trees and the internal structure details of fruit trees.

1. Introduction

Nowadays, quality is the one of the most important aspect in fruit production and marketing. Canopy structure-related variations in light interception and distribution affect productivity, yield and the quality of the harvested product (Louarn et al., 2008). Apple quality is strictly linked to light interception in the canopy. Some authors demonstrated that high quality commercial apples do not develop on areas of the tree receiving less than 50% of total incident light energy, while other authors reported that 30% of the total light is needed to ensure good yield (Corelli and Sansavini, 2015; Musacchi and Serra, 2018; Sansavini and Corelli-Grappadelli, 1997). In order to study the distribution of light interception inside the apple tree canopy, three-dimensional reconstruction techniques have been used by scientists to analyze the canopy light distribution (Sonohat et al., 2006).

Branching and connections between the plant units and their spatial location, orientation, size and shape describe the plant's architecture (Casella and Sinoquet, 2003). Leaf Spatial Location (LSL) is the leaf location in the tree canopy, that is to say, LSL gives the spatial co-ordinates of the petiole–midrib junction point (Fig. 1). To a large extent, the 3D reconstruction of the tree canopy is the 3D distribution and reconstruction of the foliage in the tree canopy, which can be achieved by combining both the spatial locations of shoots and the foliage reconstruction rules derived (Willaume et al., 2004; Yang et al., 2016).

The tree model has been conceived as a simulation algorithm that produces the forms and patterns of plants (Fisher, 2002). That is to say, computer representations of plants (virtual plants) can describe the plant architecture, or simulate the plant management process. Tree models and virtual plants are divided into two categories, tree-like models and real-tree models.

Real-tree models are aimed at generating a real tree based on measurement data, and are often used for scientific research (Fu et al.,

* Corresponding author. Tel.: +86 10 62736741.
E-mail address: pac@cau.edu.cn (G. Liu).

https://doi.org/10.1016/j.compag.2019.104975
Received 14 February 2019; Received in revised form 22 August 2019; Accepted 24 August 2019
Available online 11 September 2019
0168-1699/

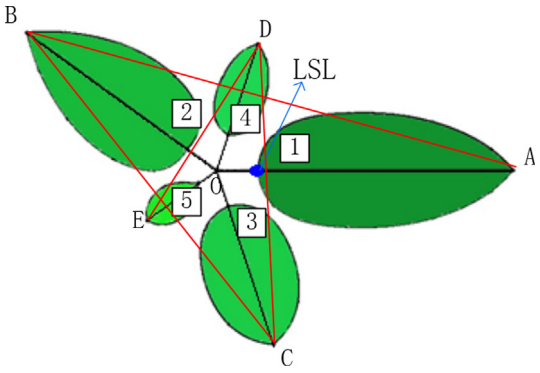

Fig. 1. Map of apple tree phyllotaxis and LSL. 1–5 are the phyllotaxis, A to E is the leaf blade apex, the blue dot is the LSL. (For interpretation of the references to color in this figure legend, the reader is referred to the web version of this article.)

2019) and to guide production practices. Simulations based on real-tree models offer the opportunity to simulate management and genotypic changes. Virtual plants are used as the basis for models simulating leaf transpiration and sap flow (Dauzat et al., 2001). The RATP (radiation absorption, transpiration and photosynthesis) model simulated the spatial distribution of carbon gain and water loss within canopies (Sinoquet et al., 2001). Researchers tested the leaf area of walnut, peach, mango, olive and rubber of the three-dimensional digitized trees (Phattaralerphong et al., 2006). The stochastic functional–structural GreenLab model, simulates plant development and growth accurately and efficiently (Kang et al., 2008). The QualiTree (Pallas et al., 2016) model provided a parsimonious model for fruit quality at the tree scale. A method for estimating light partitioning at the intra-tree canopy scale has been presented based on the three-dimensional reconstruction of the tree canopy. The VegeSTAR software can be used for the visualization of 3D plant structure, and computation of light interception and carbon acquisition by photosynthesis (Adam et al., 2004; Rakocevic et al., 2011).

The foliage and branch geometry data acquisition of these models mostly relies on manual measurements or digital instruments (Sinoquet et al., 1998; Pallas et al., 2016; Yang et al., 2017). Although these studies have made some contributions in fruit quality management, the complexity of data collection and the effort and cost of model generation limits the application of these models. In addition, branching patterns and foliage placement cannot be accurately described quickly (Bremer et al., 2013). These methods can hardly meet the requirements of leaf blade position accuracy and fast data acquisition for scientific research, such as illumination distribution (Ma et al., 2018) and light interception analysis, as well as phenotypic analysis.

With the development of measuring technologies, data acquisition methods have changed dramatically. Some approaches use a 3D time-of-flight camera integrated with a 2D camera to accomplish precise 3D point cloud registration over multiple views (Li and Tang, 2017). Although this system offers speed, accuracy, low cost and is non-destructive, which means that it can be used to collect and process data throughout the lifecycle of plants, it cannot be used in the case of large trees, such as a single 3–5 m apple tree. Consumer-grade RGB-Depth (RGB-D) cameras, such as the Kinect V2, are a low-cost option for gathering 3D point clouds. However, because of their narrow field of view (FOV), their collection efficiency and data coverage are lower than that of laser scanners (Chen and Yue, 2016). Terrestrial laser scanning (TLS) offers a unique opportunity to conduct non-invasive and non-destructive measurements (Koma et al., 2018; Pfeiffer et al., 2018; Gangadharan et al., 2019) of canopies to characterize plant growth and to analyze diverse architectural parameters. TLS measurements render point clouds that depict the surface of the visible canopy oriented towards the observing device (Wilkes et al., 2017). These point clouds can be further analyzed, with emerging applications in the fields of forest ecology, precision agriculture, and phenotyping. The application of TLS and mobile- or vehicle-based laser scanning (MLS) allows fast 3D-data acquisition. It realizes the direct capture of tree geometry, generating high resolution point measurements representing the geometrical characteristics of target objects in 3D space. Nowadays, the TLS is more and more applied to field plant phenotyping, treetop and trunk detection (Bremer et al., 2013; Mongus and Žalik, 2015), and automatic and accurate estimation of a crop's leaf area profile (Su et al., 2018).

In conclusion, to obtain the three-dimensional point cloud of a complete tree accurately and quickly and achieve reconstruction of the tree canopy, TLS is a good choice to obtain the object surface information (Pfeiffer et al., 2018). The contribution of TLS in tree skeleton extraction (Digumarti et al., 2018) and canopy holistic research (He et al., 2018) is obvious; additionally, there is some significant research in the details of each organ in the canopy (Koma et al., 2018).

The aim of the present study is to propose an automated LSL extraction methodology based on geometric relations and cluster characteristics of the 3D point clouds obtained by TLS and apply the method to automatically extract LSL from a current-year branch point clouds. We then compare the accuracy of automatic extraction and manual extraction to prove the validity and applicability of the algorithm. This study reduced the experimental time necessary for the extraction of the LSL, and improves the canopy three-dimensional reconstruction efficiency.

2. Materials and methods

2.1. Computational process overview

For this measurement setup, we implemented the following computational approach, shown in Fig. 2. Raw data that constitute the input to our system are station data obtained from TX8.

Using a series of processing steps, we used Trimble RealWorks 12.0 to transform the tree apple crown station data into spatial coordinates (Fig. 3). Then, a single branch with leaves was selected.

The following step in the progress was leaf separation from the branch (Section 2.4).

According to the law of leaf growth, leaves are centered on stems. In order to find the LSL, we need to simplify the branches into a space line, which is the branch center determination (Section 2.5).

The next step is to figure out the coordinates of the point in the leaf, with the smallest distance from the leaf to the space line, called the LSL (Section 2.6).

In the remainder of this article, we will explain the technicalities of these computational steps and demonstrate the operation of our system through experimental results obtained during a complete model acquisition and analysis process. The algorithm was developed in the MATLAB programming environment.

2.2. Tree sampling and data acquisition

The study sites were located at about east longitude 116.162°, north latitude 40.242°, and the altitude was 210.35 m. The region has a typical sub-humid continental monsoon climate with a dry windy spring, hot summer and rainy, cool autumn, cold and dry winter, and four distinct seasons. The mean minimum temperature is 11.8 °C, and the annual rainfall is about 550.3 mm, with average annual sunshine of 2684 h.

The apple cultivars were seven-year-old 'Fuji', and were grafted onto inter-stock combinations with free spindle and tall spindle training systems. The trees were planted at 2.5 × 4.5 m distances in a south–north orientation. The horticultural practice was the traditional management mode, including regular irrigation with mini-sprinklers to avoid soil water deficits, standard fertilization, and insect protection. The trees were pruned during the dormant season, not in the growing

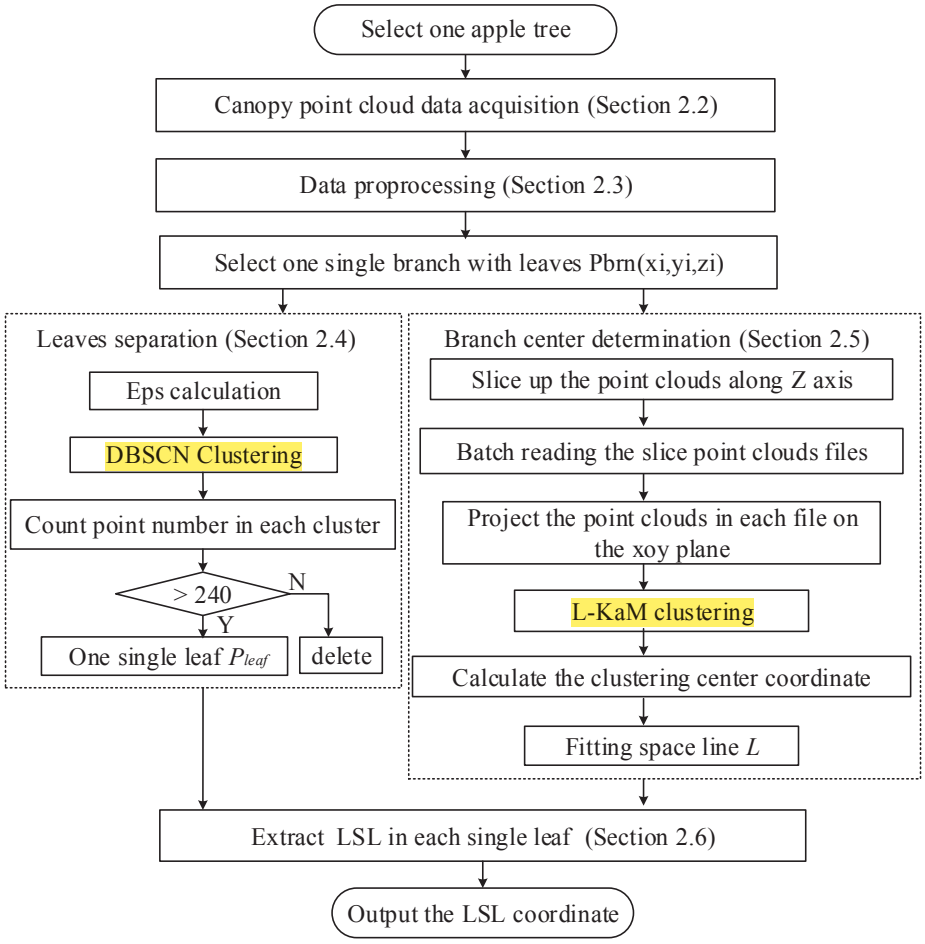

Fig. 2. The computational process for LSL extraction.

season.

For the present study, a "Trimble TX8" laser scanner (Trimble Navigation Limited Company, USA) (Fig. 2a) was used. The scanner is available with an effective scan speed of one million points per second. The number of points corresponds to the resolution of measurement. Different quality options that differ in ranging noise and scan rate at a certain resolution are available. The TX8 scanning quality parameters generally have three settings, level 1, level 2, and level 3. Under these three scanning quality settings, the space points at 30 m are 22.6 mm, 11.3 mm, and 5.7 mm apart, respectively, while the corresponding numbers of points are 34 million points (Mpts), 138 Mpts, and 555 Mpts, respectively. The Trimble TX8 maintains its high precision over the entire range of 120 m with no need to reduce speed, and the range systematic error at 100 m distance is 2 mm. The device uses a laser wavelength of 1.5 µm. The scanner can measure 360° on the vertical axis by rotation of the head of the scanner and 317° on the horizontal axis using a rotating mirror.

To accurately capture the apple tree canopy raw point cloud data, clear, calm or breezy days, with a wind speed of about 1.3 m/s (Guo et al., 2017), in May were selected. The distance used for scanning the

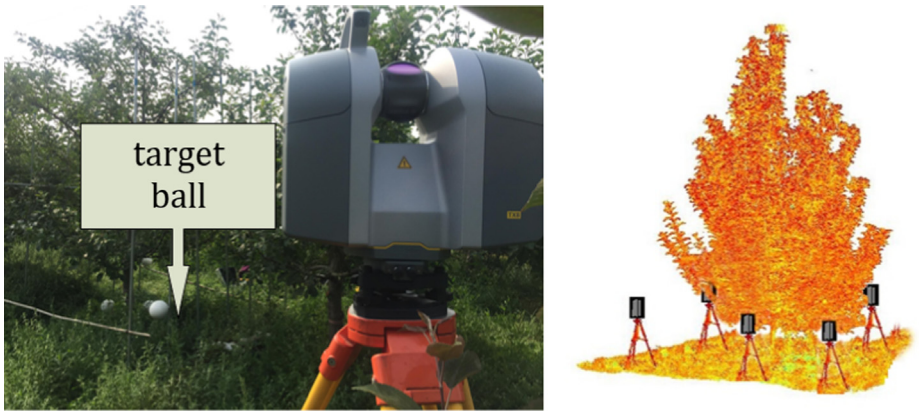

(a) Trimble TX8 and target balls (b) Five stations

Fig. 3. Terrestrial laser scanning of apple tree canopy.

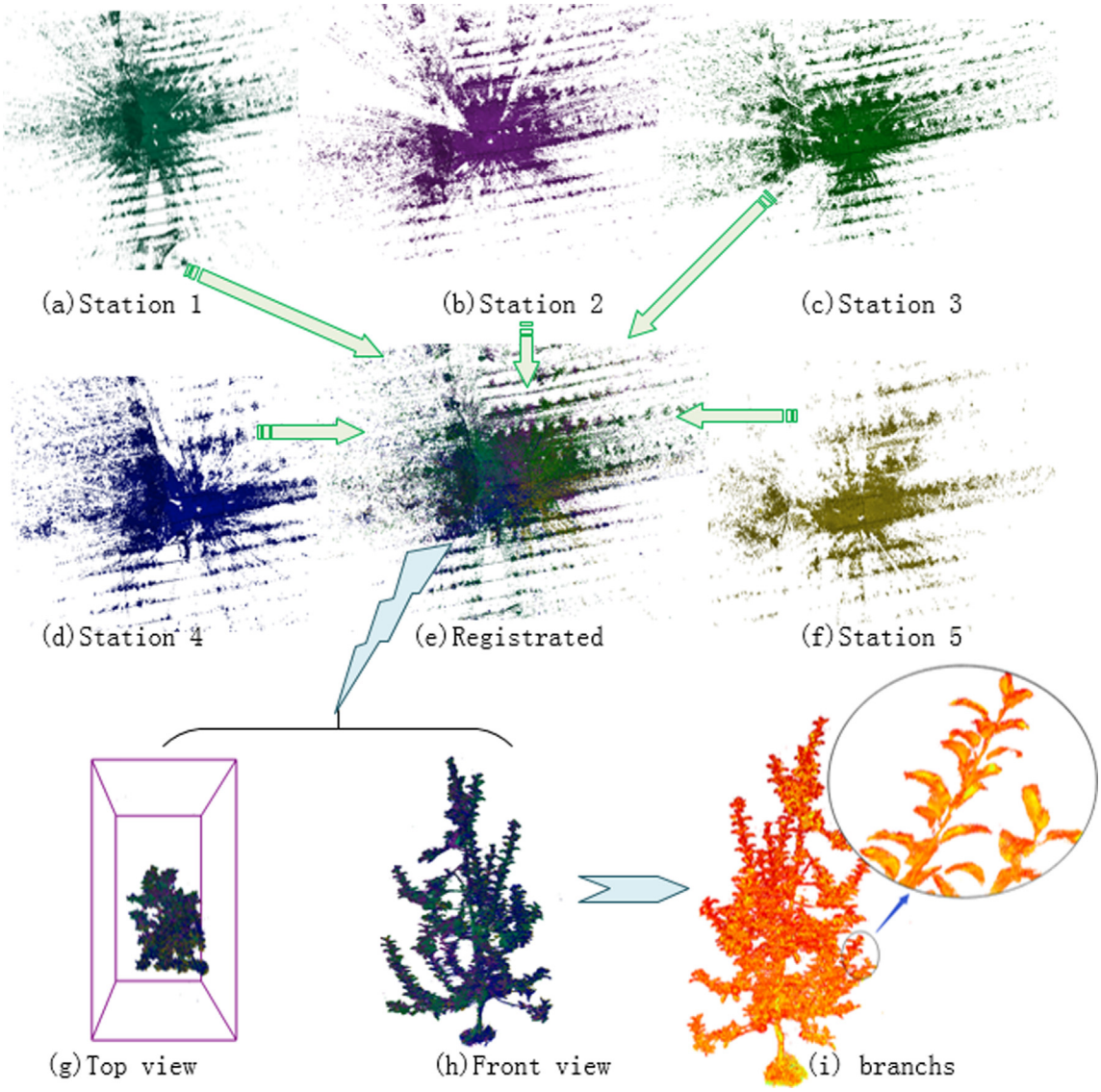

Fig. 4. The progress of obtaining the apple tree canopy point cloud.

apple tree from the Trimble TX8 (Fig. 3a) to the center of the apple tree canopy averaged 3.5 m. It took about 10 min at level 3 to complete scanning at each position and the lighting condition was set as 'outdoor conditions over entire range'. To obtain the canopy shape completely, the TX8 was placed at five stations around the canopy (Fig. 3b). Considering the different coordinate systems of different positions, 5 white target balls (Fig. 3a) with a diameter of 145 mm were placed around the canopy. It should be noted that the balls were placed at positions which were visible at each scanner station. At least three target balls could be seen by the scanner at each station.

2.3. Point cloud preprocessing

Fig. 4a, b, c, d, and f show the apple tree canopy 3D point cloud data obtained at level 3 quality using the TX8. The number of clouds per station was about 240 million. Then, the iterative closest point (ICP) algorithm (Besl and McKay, 1992; Zhang, 2014; Sobreira et al., 2019) was used to register each individual station's data into integrated and consistent point clouds of the apple tree crown. Fig. 4e shows the registered result on data from the five stations. Since ICP requires an exhaustive search through the correspondence space, the target ball was used to facilitate the registration progress.

Because of the complexity of the environment, the raw data of the apple tree canopy contain noise from various sources, such as the breeze stirring the leaves, flying insects, even dust in the air. It is therefore important to remove noise from the point cloud. We removed these points using the Geomagic Studio 2013 software (Calì et al., 2018; Boschetto et al., 2019). As the canopy has organic shape characteristics, "the free form shapes" option reduces the noise with respect to surface curvature. Fig. 4g and h show the visualization of one apple tree preprocessing result on the top and front views, respectively.

Let a single branch be defined as $P_{brnorigin}$. The number of point clouds contained in this branch is n, so $P_{brnorigin}$ is a $n \times 3$ matrix. Fig. 4i shows an example branch.

To reduce the computation and running time in the LSL extraction process, the number of point clouds needs to be reduced. The fast neighborhood search and adaptive information entropy methods (Chen and Yue, 2016) were used, and the point cloud was compressed to one tenth of the original point cloud, and it was defined as P_{brn}.P_{brn} is a matrix of size $^{n}/_{10} \times 3$. The i-th point's spatial coordinates are $P_{brni}(x_{brnii}, y_{brni}, z_{brni})$.

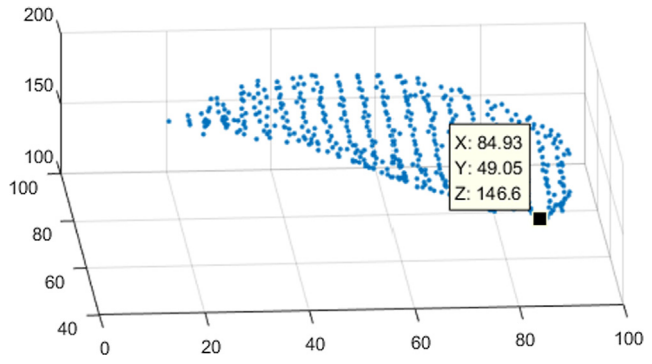

Fig. 5. Space coordinates of LSL.

2.4. Leaf separation

The leaf point cloud can be separated from the branch point cloud of the registered point cloud because there is a typical point density within each leaf or branch, which is much higher than the outer parts of the leaf or branch, or the space contour formed by the point and the surrounding is different.

Cluster analysis is aimed at classifying elements into categories on the basis of their similarity. In this paper, we used density-based spatial clustering of applications with noise (DBSCAN) (Mahesh Kumar and Rama Mohan Reddy, 2016, Martin Ester Jörg and Xiaowei, 2012) as the primary data analysis method to process the point cloud data. Given a set of points in some space, DBSCAN groups together points that are closely packed together, marking them as the same cluster. Points that lie alone in low-density regions, are marked as outliers.

For DBSCAN clustering, two parameters are important: *Eps*, which is defined as the maximum radius of the neighborhood and *Minpts*, which is defined as the number of points.

The given points areP_{brn}, and the parameters *Minpts* and *Eps* needed are determined by the characteristics of P_{brn} according to the linear relationship between the distance from the scanner to the object being measured and the distance of the scanning points (Chenet et al., 2016). During development, by taking into account the scan settings described in Section 2.1, we calculated *Eps* according to Eq. (1):

$$Eps = G_{ridstep} \times \frac{L}{Q} \tag{1}$$

where L is the distance from the scanner to the object being measured. $G_{ridstep}$ is the grid step in the point cloud after compression. Q is the value related to the scan quality parameter setting. After calculation, *Eps* is about 5.8 and *Minpts* is equal to 4.

In this paper, in order to reduce computations and program running time, the K-Nearest Neighbor (Peterson, 2010) algorithm was adopted to find the nearest neighbor in $P_{brn}$for each point by Euclidean distance.

The leaf separation process starts by selecting an unvisited point $(x_0, y_0, z_0) \in P_{brn}$ at random and finding its *Eps*-neighborhood$(x_n, y_n, z_n) \in P_{brn}$. Then, if $\|(x_0, y_0, z_0) - (x_n, y_n, z_n)\| \leqslant Eps$, the point (x_n, y_n, z_n) is marked as an *Eps*-connected point. If $\sqrt{(x_0 - x_n)^2 + (y_0 - y_n)^2 + (z_0 - z_n)^2} \leqslant Eps$, the point (x_n, y_n, z_n) is marked as an *Eps*-neighborhood point. Initially, all points are marked as unvisited.

If the number of points in its eps-neighborhood is less than *Minpts*, then it is marked as noise or an outlier, otherwise a new cluster is created. If no unvisited points can be added to cluster, the new cluster is complete and no points will be added to the cluster in subsequent iterations.

When counting the points present in each cluster, if the number of points is more than 240, the cluster was considered a single leaf; otherwise, the cluster is deleted. This means that a single leaf has been obtained. The process is completed when all the points are either assigned to some cluster or marked as noise.

2.5. Branch center determination

This section provides a new framework for fitting space lines based on the point cloud. The method proposed for finding the space lines of the branch is called layer K-means and median (L-KaM). To find the center of the branch, our idea was to slice the branch point clouds into layers along one direction, and then use the K-mean method to find the cluster center of each point cloud slice, and the medial method to fit a straight line. The center direction is defined as the fitting line of the center of each slice. In the initial step of the method, we choose the same branch point clouds P_{brn} as in Section 2.4.

Generally, the angle between the branches and the vertical ground direction, represented by ϕ, is between 0° and 90°. Usually, ϕ of the new branches growing in the current year will be less than 80° (Casella and Sinoquet, 2003). In the process of fitting the space line, we slice P_{brn} along the Z axis direction at 5 mm intervals. Each layer's point clouds form a point clouds group S_i, $S_i \in P_{brn}(i = 1, 2, 3. ..)$, where i is the slice number. Then, after reading each S_i and projecting the points on a plane *xoy*, which is perpendicular to the Z axis, we obtain the projection of S_i point clouds, denoted as S_{Pi}.

The K-means algorithm is one of the best known, benchmarked and simplest clustering algorithms (Saxena et al., 2017). For our purposes, according to the law of leaf growth, in each layer of 5 mm thickness of the branches, the number of leaves per layer does not exceed 3, so in the initial clustering section, the initial cluster centroid k is set to 3. The objective function J is the following:

$$MinimizeJ = \sum_{i=1}^{n}\sum_{i=1}^{n} \|x_i^{(j)} - c_j\|^2 \tag{2}$$

where $\|x_i^{(j)} - c_j\|^2$is a chosen distance measure between a data point $x_i^{(j)}$ and the cluster centre c_j.

The clustering center coordinates are recorded during the running of the clustering algorithm. The center coordinate consists of the x and y coordinate components. To form the two-dimensional array of cluster center coordinates, C_{2D}, we set the number of cluster center coordinates to m. That is to say,

$$C_{2D} = \begin{pmatrix} x_m & y_m \\ \cdots & \cdots \\ x_1 & y_1 \end{pmatrix}$$

A one-dimensional vector C_a is also created, with a length equal to the number of C_{2D} array rows. The value of C_a is the Z value of the projection plane of the point cloud layer.

$$C_a = \begin{pmatrix} z_m \\ \cdots \\ z_1 \end{pmatrix}$$

Then, we combined C_{2D} and C_a to form a three-dimensional array $C_{3D.}$

$$C_{3D} = \begin{pmatrix} x_m & y_m & z_m \\ \cdots & \cdots & \cdots \\ x_1 & x_2 & x_3 \end{pmatrix}$$

Each line data of C_{3D} represented the coordinates of a point in a three-dimensional space. We then iteratively calculate the median value of three adjacent points. The iteration stops until all remaining points have been processed, and the algorithm outputs the two points, $P_{CA}(x_{CA}, y_{CA}, z_{CA})$ and $P_{CB}(x_{CB}, y_{CB}, z_{CB})$.

The equation of the space line L is as follows:

$$\frac{x - x_{CA}}{m} = \frac{y - y_{CA}}{n} = \frac{z - z_{CA}}{p} = t \tag{3}$$

where (x,y, z)are any point coordinates in line L, (m, n, p) is the direction vector of the line$L$, and t is the parameter of line$L$.

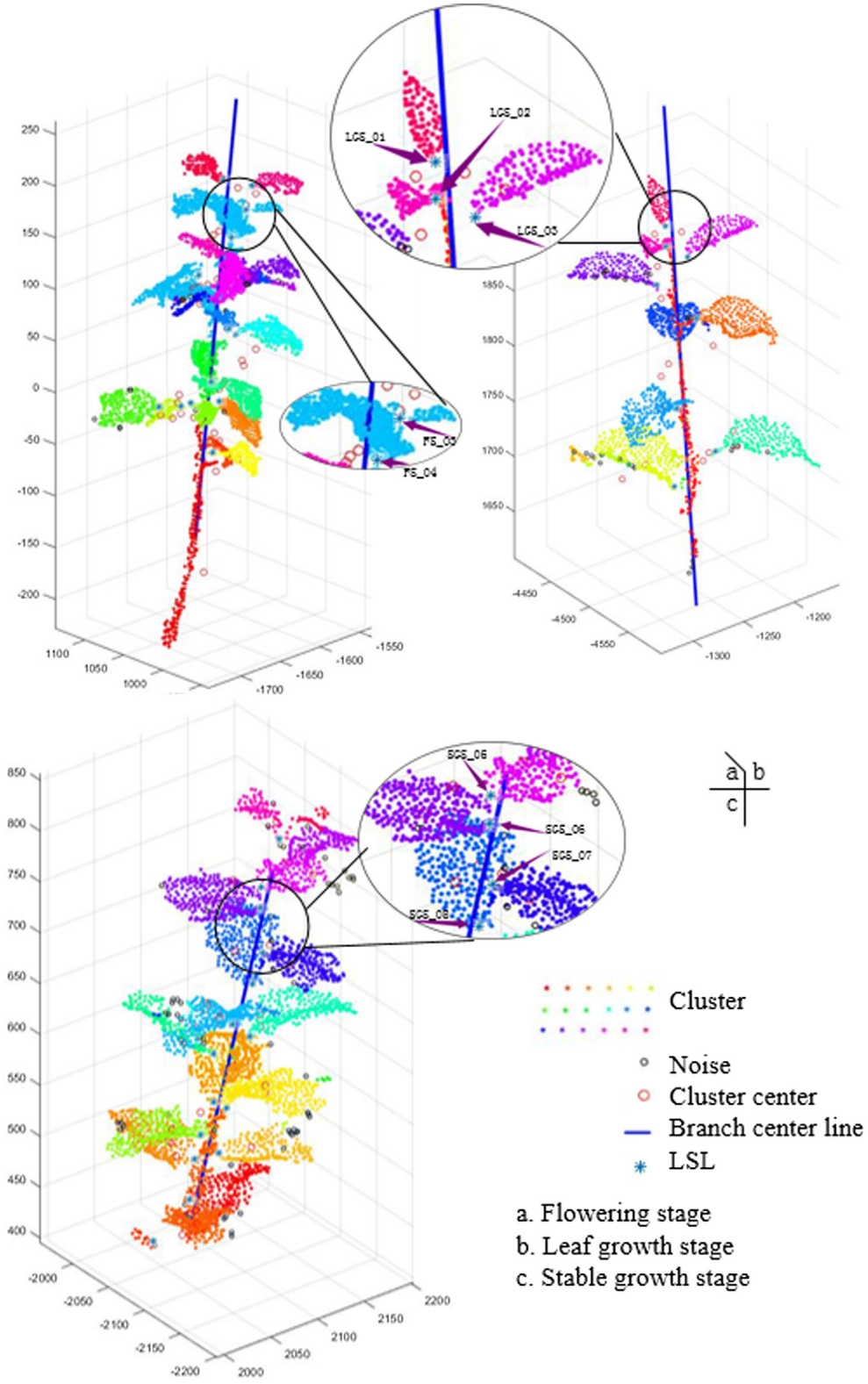

Fig. 6. LSL extraction results at different growth stages.

2.6. Finding the LSL

The leaf point cloud $P_{leaf}(X_{Lr}, Y_{Lr}, Z_{Lr})$ is used to find the Euclidean distance of each point in the cloud to line L. The calculation equation is as follows:

$$d(P_{leafi}, L) = \frac{\left\| \begin{matrix} \vec{i} & \vec{j} & \vec{k} \\ x_{CA} - X_{Lri} & y_{CA} - Y_{Lri} & z_{CA} - Z_{Lri} \\ m & n & p \end{matrix} \right\|}{\|m, n, p\|} \quad (4)$$

where $d(P_{leafi}, L)_{\min}$ is the minimum Euclidean distance, and on the leaf

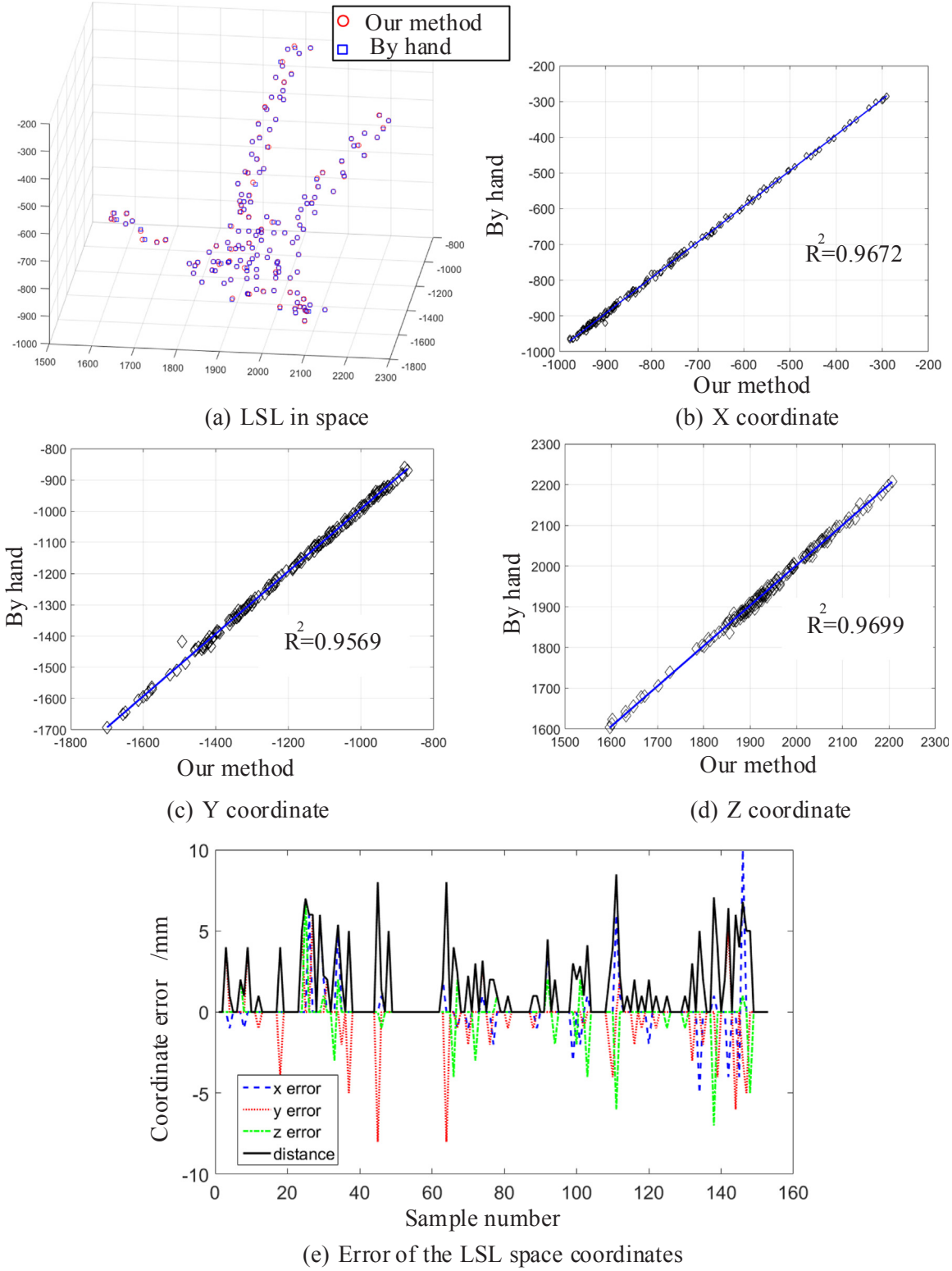

Fig. 7. Comparison of two LSL extraction methods.

corresponding to the minimum Euclidean distance is the LSL point. Fig. 5 shows the space coordinates of the LSL.

3. Results and discussion

3.1. LSL extraction results

Using the method designed in this paper, a 4-year-old spindle training system apple tree was taken as the research object, and three-dimensional point cloud data at the flowering stage (FS), Leaf growth

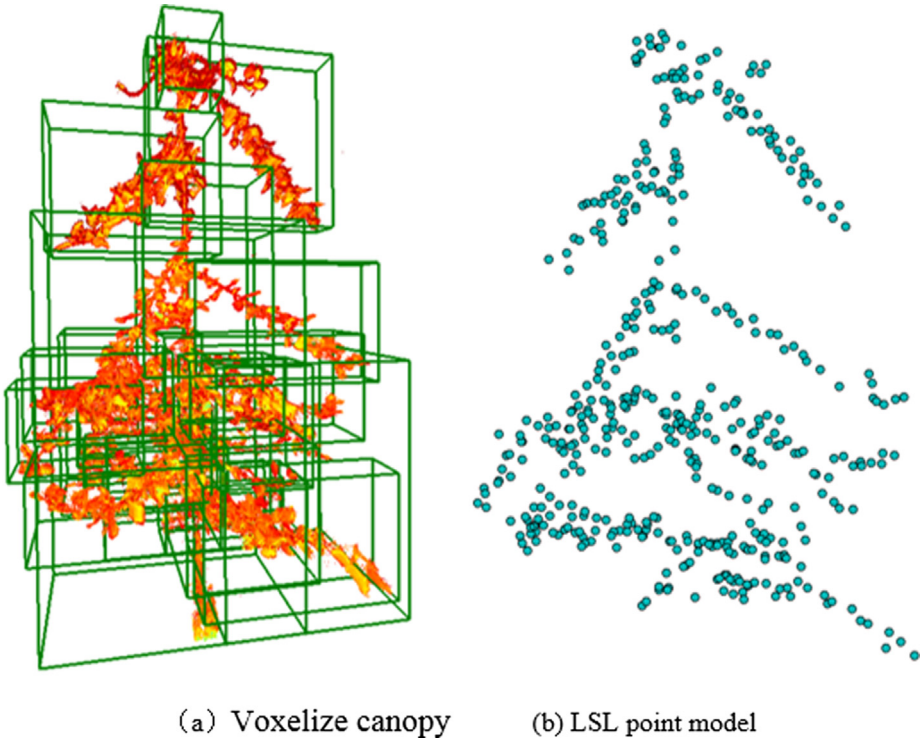

Fig. 8. LSL point model.

Table 1
Comparison of the correct extraction rates.

Sample tree	Canopy Point number	Average point number of single leaf	Leaf number	LSL number	Correct extraction rate/%
VD-3a -1	391,608	294	1332	1222	91.71
VD-3a -2	561,246	294	1909	1532	80.21
VD-3a -3	280,476	294	954	934	97.80
VV-3a -1	656,125	287	2286	1599	69.94
VV-3a -2	591,224	287	2060	1501	72.86
VV-8a-1	5,134,564	355	14,463	4210	29.11
VV-8a -2	5,143,432	355	14,488	4351	30.03
VV-8a -3	1,199,338	355	3378	1920	56.83

stage (LGS) and stable growth stage (SGS) were extracted.

It can be seen from Fig. 6 that the method can extract the LSL of the shoots in different growth stages of spindle training system apple trees. The different colors in the Fig. 6 represent different sets of three-dimensional points, and different colors represent different leaves. Because there are no new branches growing in the canopy of the fruit-bearing tree during the flowering period, there are perennial branches, flower bones and petals in the canopy. The 3D point cloud quality acquired through TLS is affected by the plush and petals of the surface of the young leaves, and the 3D point cloud of the leaves and branches is not obtained correctly. Fig. 6(a) is the result of branch LSL extraction during the flowering stage. It can be seen from the figure that there are more noise points at the corners of the leaves and branches, which are caused by tender leaves and flowers. The method proposed in this paper cannot segment leaves from branches more accurately, as a plurality of leaves forms a set of point clouds, so distinguishing a single blade from those point clouds is a difficult task. The accuracy of LSL is also poor and FS_03 and FS_04 were not the real LSLs. Fig. 6(b) and (c) are the results of LSL extraction at the leaf growth and stable growth stages, respectively. These two growth stage are the stages in which the canopy rapidly increases the volume of the canopy. The blade of the leaves are grown, the organs in the canopy were relatively simple, the leaves can be accurately segmented, and the LSL can be extracted, as shown by LGS_01, LGS_02, LGS_03 in Fig. 6(b), and SGS_05, SGS_06, SGS_07 and SGS_08 in Fig. 6(c).

3.2. LSL coordinate accuracy

Fig. 7 shows a comparison of LSL manual test points by Realworks software and automatically generated points for some branches belonging to a 3-year-old high-spindle training apple canopy in August 2017. Red circles in Fig. 7(a) represent the LSL position automatically determined by our method, and blue rectangles represent the manual measurements of the LSL position. The coincidence of circles and rectangles indicates that there was no error in the measurement point.

To verify the accuracy of extracting LSL coordinates using our method, the LSL coordinates in our method were validated with the manual measurement values using regression methods. It should be noted that a significant linear relationship arises of x, y and z coordinates between the two methods as illustrated in Fig. 7(b), (c) and (d). The R^2 were 0.9672, 0.9569, 0.9699 respectively.

In order to represent the magnitude of the error value, Fig. 7(e) shows the error values of the three coordinates of the manual test point and the automatically generated LSL's x, y, z space coordinates and the ELD_MaA value. It can be seen that the average errors of x, y, z coordinates were 0.15 mm, 0.24 mm, and 0.12 mm, respectively. The average ELD_MaA was 1.41 mm.

3.3. LSL coordinate adaptability

In this paper, to verify the LSL adaptability to different tree shape canopies, three tall spindle training system apple trees (VD) canopy (3-year-old) and five free spindle training system apple tree (VV) canopies (two 3-year-old and three 8-year-old), in their stable growth stage, were used as the research objects, respectively. Before the canopy LSL is extracted by our method, the canopy is first voxelized according to the branches, and then, the LSL extracted from each voxel were synthesized together to make a LSL point model. Fig. 8a shows a visualization of the

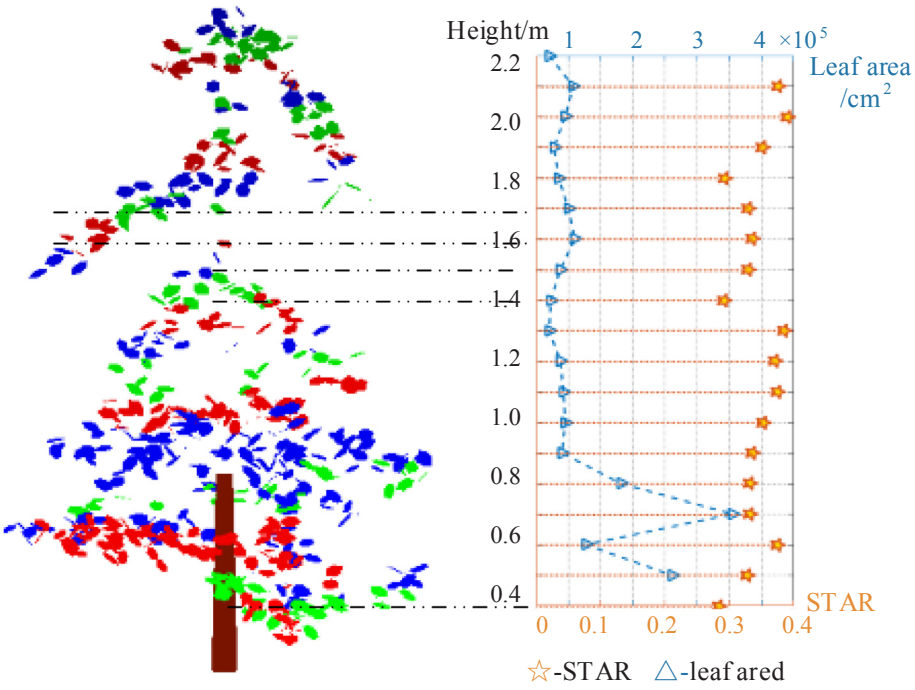

Fig. 9. LSL Point model with VegeSTAR fusion calculation canopy STAR.

point clouds data of voxel apple canopy, and Fig. 8b shows the LSL extracted from the canopy. It can be seen that, the LSL extracted in the Fig. 8b has a better effect in the sparsely branched areas, while the LSL number extracted in the deep and lower part of the canopy, is less than the actual quantity, and the extraction accuracy is shown in Table 1.

From Table 1, the data shows that, the point clouds number in VV canopy and VD are different. According to the same scanning setting and point cloud processing method, the number of canopy point clouds and the average number of leaf point clouds can be obtained, and then the number of leaves in the canopy can be obtained. The ratio of the number of LSL extracted according by our method to the total number of canopy leaves is the correct extraction accuracy. The data in the table shows that, the LSL correct extraction rate of VD is higher than that of VV, and the average extraction rate of VD and VV is 89.90% and 51.75%, respectively. VD and VV of the same age, the number of VV point clouds is more than VD, and the correct extraction efficiency is lower than VD, which is 71.40% and 89.90%, respectively. The VV of different ages, the larger the number of clouds, the lower the correct extraction rate. The correct extraction rates of 3 year tree and 8 year tree were 71.4% and 38.66%, respectively, which was 32.74% lower.

3.4. LSL coordinate application

VegeSTAR is a popular light interception calculation model (Westling et al., 2018) in tree analysis (Rakocevic et al., 2011; Rakocevic and Androcioli-Filho, 2010). With this model, the LSL point model established by our method can perform light interception analysis. Fig. 9 shows the LSL point model with the VegeSTAR fusion calculation canopy STAR (Silhouette to Total Area Ratio). The canopy model was cut into 10 cm sections in the height direction of the tree. VegeSTAR can calculate the leaf area and STAR at different heights in the vertical direction of the canopy. The user even can remove some of the LSL points to simulate pruning and perform light interception analysis. The model can also be applied for pruning recommendation towards automated orchard decision support and management.

The method for apple tree branch LSL extraction is conceptually simple but effective. It can obtain the canopy LSL value in a short time compared to manual extraction (Wei-Wei et al., 2014). The manual extraction-reconstructed 1500-point crown 3D model takes about 2 days, while the LSL point model takes about 2.5–3 h, which corresponds to a 8 times increase in efficiency.

4. Conclusion

In this study, a method of extracting the base points of fruit branches by using point cloud and multi-cluster is proposed. The innovation of this method is to accurately separate the leaves in the branches, and use the point cloud and multi-cluster to obtain the the center of the branches. The method designed and tested in this paper can extract the LSL from apple tree canopy 3D point cloud data. The LSL coordination accuracy achieved using our method has been validated using hand extraction by Realworks with satisfactory performance, which shows that our method can be a suitable alternative for 3D reconstruction.

Using TLS, we acquired point clouds data in the FS, LGS and SGS tree growth stages, respectively. Due to the flower bone and the bud on the FS branches, LSL was difficult to be extracted. Therefore, the method proposed in this paper is applicable to LGS and SGS. The experimental results revealed that the LSL was successfully extracted using the method in our study, with average x, y, z coordinate errors of 0.15 mm, 0.24 mm, and 0.12 mm, respectively, and an average ELD_MaA of 1.41 mm.

The LSL correct extraction rate of VD was higher than that of VV, with the corresponding average extraction rates being 89.90% and 51.75%, respectively.

This method shortens the calculation time and improves the accuracy of fruit tree leaf information, obtaining the whole apple tree's (3-year-old) LSL value about 2.5–3 h, corresponding to a 8-time efficiency increase over manual methods.

It is valuable for human interaction with data, canopy data visualization, automated analysis, such as calculating leaf area index, and illumination distribution. The research results form the foundation for analyzing the light intensity distribution inside the fruit tree canopy.

In the future, we will focus on the automatic LSL extraction for more kinds of trees, such as pear trees, peach trees, etc. The problem of missing point cloud data in deep canopies due to leaf occlusion, and improving the correct extraction rate is still a difficult problem.

Declaration of Competing Interest

The authors declare no conflict of interest. The founding sponsors had no role in the design of the study; in the collection, analyses or interpretation of the data; in the writing of the manuscript; nor in the decision to publish the results.

Acknowledgements

This project was supported by a grant from the National Key Research and Development Project [Grant No. 2017YFD0700503], and by the Foundation of Key Laboratory of Modern Agricultural Equipment and Technology, Ministry of Education. At the same time, it was supported by the Colleges and universities in Hebei province science and technology research projects [Grant No. QN2017417] and the Hebei Provincial Natural Science Foundation [Grant No. C2015204043] participated in program debugging.

Appendix A. Supplementary material

Supplementary data to this article can be found online at https://doi.org/10.1016/j.compag.2019.104975.

References

Adam, B., Dones, N., Sinoquet, H., 2004. VegeSTAR v.3.1. A software to compute light interception and photosynthesis by 3D plant mock-ups. In: 4th Int. Work. Functional-Structural Plant Model, pp. 414..

Besl, P.J., McKay, N.D., 1992. A method for registration of 3-D shapes. IEEE Trans. Pattern Anal. Mach. Intell. https://doi.org/10.1109/34.121791.

Boschetto, A., Bottini, L., Costanza, G., Tata, M.E., 2019. Shape memory activated self-deployable solar sails: small-scale prototypes manufacturing and planarity analysis by 3D Laser Scanner. Actuators. https://doi.org/10.3390/act8020038.

Bremer, M., Rutzinger, M., Wichmann, V., 2013. Derivation of tree skeletons and error assessment using LiDAR point cloud data of varying quality. ISPRS J. Photogramm. Remote Sens. 80, 39–50. https://doi.org/10.1016/j.isprsjprs.2013.03.003.

Calì, M., Zanetti, E.M., Oliveri, S.M., Asero, R., Ciaramella, S., Martorelli, M., Bignardi, C., 2018. Influence of thread shape and inclination on the biomechanical behaviour of plateau implant systems. Dent. Mater. https://doi.org/10.1016/j.dental.2018.01.012.

Casella, E., Sinoquet, H., 2003. A method for describing the canopy architecture of coppice poplar with allometric relationships. Tree Physiol. 23, 1153–1170. https://doi.org/10.1093/treephys/23.17.1153.

Chen, Y., Yue, L., 2016. A method for dynamic simplification of massive point cloud. In: Proc. IEEE Int. Conf. Ind. Technol. 2016-May, pp. 1690–1693. https://doi.org/10.1109/ICIT.2016.7475017.

Corelli, L., Sansavini, S., 2015. Light interception and photosynthesis related to planting density and canopy management in apple. Acta Hortic. https://doi.org/10.17660/actahortic.1989.243.20.

Dauzat, J., Rapidel, B., Berger, A., 2001. Simulation of leaf transpiration and sap flow in virtual plants: model description and application to a coffee plantation in Costa Rica. Agric. For. Meteorol. 109, 143–160. https://doi.org/10.1016/S0168-1923(01)00236-2.

Digumarti, S.T., Nieto, J., Cadena, C., Siegwart, R., Beardsley, P., 2018. Automatic segmentation of tree structure from point cloud data. IEEE Robot. Autom. Lett. 3, 3043–3050. https://doi.org/10.1109/lra.2018.2849499.

Fisher, J.B., 2002. How predictive are computer simulations of tree architecture? Int. J. Plant Sci. https://doi.org/10.1086/297071.

Fu, L., Tola, E., Al-Mallahi, A., Li, R., Cui, Y., 2019. A novel image processing algorithm to separate linearly clustered kiwifruits. Biosyst. Eng. https://doi.org/10.1016/j.biosystemseng.2019.04.024.

Gangadharan, S., Burks, T.F., Schueller, J.K., 2019. A comparison of approaches for citrus canopy profile generation using ultrasonic and Leddar® sensors. Comput. Electron. Agric. https://doi.org/10.1016/j.compag.2018.10.041.

Guo, C., Zong, Z., Zhang, X., Liu, G., 2017. Apple tree canopy geometric parameters acquirement based on 3D point clouds. Nongye Gongcheng Xuebao/Trans. Chin. Soc. Agric. Eng. https://doi.org/10.11975/j.issn.1002-6819.2017.03.024.

He, G., Yang, J., Behnke, S., 2018. Research on geometric features and point cloud properties for tree skeleton extraction. Pers. Ubiquitous Comput. 22, 903–910. https://doi.org/10.1007/s00779-018-1153-2.

Kang, M.Z., Cournède, P.H., de Reffye, P., Auclair, D., Hu, B.G., 2008. Analytical study of a stochastic plant growth model: application to the GreenLab model. Math. Comput. Simul 78, 57–75. https://doi.org/10.1016/j.matcom.2007.06.003.

Koma, Z., Rutzinger, M., Bremer, M., 2018. Automated segmentation of leaves from deciduous trees in terrestrial laser scanning point clouds. IEEE Geosci. Remote Sens. Lett. 15, 1456–1460. https://doi.org/10.1109/LGRS.2018.2841429.

Li, J., Tang, L., 2017. Developing a low-cost 3D plant morphological traits characterization system. Comput. Electron. Agric. 143, 1–13. https://doi.org/10.1016/j.compag.2017.09.025.

Louarn, G., Lecoeur, J., Lebon, E., 2008. A three-dimensional statistical reconstruction model of grapevine (*Vitis vinifera*) simulating canopy structure variability within and between cultivar/training system pairs. Ann. Bot. https://doi.org/10.1093/aob/mcm170.

Ma, X., Feng, J., Guan, H., Liu, G., 2018. Prediction of chlorophyll content in different light areas of apple tree canopies based on the color characteristics of 3d reconstruction. Remote Sens. 10. https://doi.org/10.3390/rs10030429.

Mahesh Kumar, K., Rama Mohan Reddy, A., 2016. A fast DBSCAN clustering algorithm by accelerating neighbor searching using Groups method. Pattern Recogn. 58, 39–48. https://doi.org/10.1016/j.patcog.2016.03.008.

Martin Ester Jörg, S., Xiaowei Xu, H.K., 2012. CiteSeerX – A density-based algorithm for discovering clusters in large spatial databases with noise. doi:10.1.1.71.1980.

Mongus, D., Žalik, B., 2015. An efficient approach to 3D single tree-crown delineation in LiDAR data. ISPRS J. Photogramm. Remote Sens. 108, 219–233. https://doi.org/10.1016/j.isprsjprs.2015.08.004.

Musacchi, S., Serra, S., 2018. Apple fruit quality: overview on pre-harvest factors. Sci. Hortic. (Amsterdam). https://doi.org/10.1016/j.scienta.2017.12.057.

Pallas, B., Da Silva, D., Valsesia, P., Yang, W., Guillaume, O., Lauri, P.E., Vercambre, G., Génard, M., Costes, E., 2016. Simulation of carbon allocation and organ growth variability in apple tree by connecting architectural and source-sink models. Ann. Bot. https://doi.org/10.1093/aob/mcw085.

Peterson, L., 2010. K-nearest neighbor. Scholarpedia. https://doi.org/10.4249/scholarpedia.1883.

Pfeiffer, S.A., Guevara, J., Cheein, F.A., Sanz, R., 2018. Mechatronic terrestrial LiDAR for canopy porosity and crown surface estimation. Comput. Electron. Agric. 146, 104–113. https://doi.org/10.1016/j.compag.2018.01.022.

Phattaralerphong, J., Sathornkich, J., Sinoquet, H., 2006. A photographic gap fraction method for estimating leaf area of isolated trees: assessment with 3D digitized plants. Tree Physiol. 26, 1123–1136. https://doi.org/10.1093/treephys/26.9.1123.

Rakocevic, M., Androcioli-Filho, A., 2010. Morphophysiological characteristics of (*Coffea arabica* L.) in different arrangements: lessons from 3D virtual plant approach. Coffee Sci.

Rakocevic, M., Costes, E., Assad, E.D., 2011. Structural and physiological sexual dimorphism estimated from three-dimensional virtual trees of yerba-mate (Ilex paraguariensis) is modified by cultivation environment. Ann. Appl. Biol. 159, 178–191. https://doi.org/10.1111/j.1744-7348.2011.00484.x.

Sansavini, S., Corelli-Grappadelli, L., 1997. Yield and light efficiency for high quality fruit in apple and peach high density planting. Acta Horticult. https://doi.org/10.17660/ActaHortic. 1997.451.65.

Saxena, A., Prasad, M., Gupta, A., Bharill, N., Patel, O.P., Tiwari, A., Er, M.J., Ding, W., Lin, C.T., 2017. A review of clustering techniques and developments. Neurocomputing 267, 664–681. https://doi.org/10.1016/j.neucom.2017.06.053.

Sinoquet, H., Le Roux, X., Adam, B., Ameglio, T., Daudet, F.A., 2001. RATP a model for simulating the spatial distribution of radiation absortion traspiratons and photosynthesis within canopies. Plant, Cell Environ. 24, 395–406.

Sinoquet, H., Thanisawanyangkura, S., Mabrouk, H., Kasemsap, P., 1998. Characterization of the light environment in canopies using 3D digitising and image processing. Ann. Bot. 82, 203–212. https://doi.org/10.1006/anbo.1998.0665.

Sobreira, H., Costa, C.M., Sousa, I., Rocha, L., Lima, J., Farias, P.C.M.A., Costa, P., Moreira, A.P., 2019. Map-matching algorithms for robot self-localization: a comparison between perfect match, iterative closest point and normal distributions transform. J. Intell. Robot. Syst. Theory Appl. https://doi.org/10.1007/s10846-017-0765-5.

Sonohat, G., Sinoquet, H., Kulandaivelu, V., Combes, D., Lescourret, F., 2006. Three-dimensional reconstruction of partially 3D-digitized peach tree canopies. Tree Physiol. https://doi.org/10.1093/treephys/26.3.337.

Su, W., Zhu, D., Huang, J., Guo, H., 2018. Estimation of the vertical leaf area profile of corn (Zea mays) plants using terrestrial laser scanning (TLS). Comput. Electron. Agric. 150, 5–13. https://doi.org/10.1016/j.compag.2018.03.037.

Wei-Wei, Y., Xi-Long, C., Hang-Kong, L., Man-Rang, Z., Dong, Z., Ming-Yu, H., et al., 2014. Three-dimensional simulation of canopy structure and light interception for tall spindle shape of spur â€fuji'apple with dwarf interstock. Scientia Agricultura Sinica.

Westling, F., Underwood, J., Örn, S., 2018. Light interception modelling using unstructured LiDAR data in avocado orchards. Comput. Electron. Agric. https://doi.org/10.1016/j.compag.2018.08.020.

Wilkes, P., Lau, A., Disney, M., Calders, K., Burt, A., Gonzalez de Tanago, J., Bartholomeus, H., Brede, B., Herold, M., 2017. Data acquisition considerations for Terrestrial Laser Scanning of forest plots. Remote Sens. Environ. https://doi.org/10.1016/j.rse.2017.04.030.

Willaume, M., Lauri, P.É., Sinoquet, H., 2004. Light interception in apple trees influenced by canopy architecture manipulation. Trees - Struct. Funct. 18, 705–713. https://doi.org/10.1007/s00468-004-0357-4.

Yang, W., Chen, X., Zhang, M., Gao, C., Liu, H., Saudreau, M., Costes, E., Han, M., 2017. Light interception characteristics estimated from three-dimensional virtual plants for two apple cultivars and influenced by combinations of rootstocks and tree architecture in Loess Plateau of China. Acta Hortic. 1160, 245–252. https://doi.org/10.17660/ActaHortic. 2017.1160.36.

Yang, W.W., Chen, X.L., Saudreau, M., Zhang, X.Y., Zhang, M.R., Liu, H.K., Costes, E., Han, M.Y., 2016. Canopy structure and light interception partitioning among shoots estimated from virtual trees: comparison between apple cultivars grown on different interstocks on the Chinese Loess Plateau. Trees - Struct. Funct. 30, 1723–1734. https://doi.org/10.1007/s00468-016-1403-8.

Zhang, Z., 2014. Iterative Closest Point (ICP). In: Computer Vision. https://doi.org/10.1007/978-0-387-31439-6_179.